Adult lifespan trajectories of neuromagnetic signals and interrelations with cortical thickness

Christina Stier[1*], Christoph Braun[2, 3], Niels K. Focke[1*]

[1] *Clinic of Neurology, University Medical Center Göttingen, Göttingen, Germany*
[2] *MEG-Center, Hertie Institute for Clinical Brain Research, University of Tübingen, Tübingen, Germany*
[3] *CIMeC, Center for Mind/Brain Sciences, University of Trento, Rovereto, Italy*

Oscillatory power and phase synchronization map neuronal dynamics and are commonly studied to describe the healthy or diseased brain. Yet, little is known about the course of these features from early adulthood into old age. Leveraging magnetoencephalography (MEG) resting-state data in a cross-sectional adult sample (n = 350), we probed lifespan differences (18-88 years) in connectivity and power and interaction effects with sex. Building upon recent attempts to link structure and function in the brain, we tested the spatial correspondence of age effects on cortical thickness and those on functional networks and a direct relationship at the level of the study sample. We found MEG frequency-specific patterns for lower- and higher-order brain regions and divergence between sexes in low frequencies. Connectivity and power exhibited distinct linear trajectories with age or turning points at midlife. Variability in cortical thickness with age corresponded to those in neuromagnetic activity, particularly in delta and beta oscillations, and showed coupling in either unimodal or transmodal regions depending on the frequency. Altogether, we provide a comprehensive overview of the topographic functional profile of adulthood that can form a basis for neurocognitive and clinical investigations. This study further sheds new light on how the brain's structural architecture relates to fast oscillatory activity in large-scale networks.

Keywords: magnetoencephalography, resting-state, functional connectivity, structure-function coupling

*Corresponding authors: christina.stier@med.uni-goettingen.de; nfocke@uni-goettingen.de

Introduction

Brain development and aging are subject to highly complex processes that are shaped by genetic and environmental influences and are critical factors in health and disease. The onset of various disorders often coincides with specific age windows, indicating alterations in developmental or aging pathways and genetic factors. For example, genetic epilepsies and psychiatric disorders such as schizophrenia occur in childhood or adolescence, while neurodegenerative diseases like Alzheimer's disease typically emerge in the last decades of life. These pathological states are all characterized by aberrant neuronal activity and synchronization that can be measured using MEG (1-6). Thus, understanding normative brain maturation and aging based on neuronal activity is key to estimating pathological trajectories. To date, functional brain alterations across the entire lifespan have been studied primarily with fMRI. A gradual consolidation of brain networks is attributed to the early development stages, with association hubs becoming more strongly connected until adulthood (7). With old age, functional connectivity within brain networks as studied using fMRI, appears to decrease, particularly in the default mode network (DMN), and relates to cognitive decline (8, 9). These findings are thought to be in line with the hypothesis of a longer maturation period for association cortices than for primary cortices (9-12) and the particular vulnerability of these cortices to developmental disruption (13). Other fMRI networks such as attention, salience, or motor networks also appear to be impacted during the life course, but the evidence is inconclusive (8, 14-16). Importantly, cerebrovascular function changes with age and can substantially confound fMRI connectivity measures if not corrected appropriately (17). MEG, on the other hand, is less sensitive to vascular confounds (17), measures neuronal activity more directly than fMRI and can capture fast neuronal dynamics. Hence, it is of great interest to track the brain's functional profile across the lifespan using electrophysiology, which has been extensively used in clinical and cognitive neuroscience (18). Previous seminal studies have focused on specific age ranges (19-22) or were done at the scalp level (23, 24), limiting the spatial specificity and possibility of studying anatomically distributed networks. Hence, our goal was to investigate regional variability of oscillatory activity during adulthood and the resting-state using source reconstruction methods, resolved for six conventional frequency bands. Based on earlier reports (23), we expected linear and non-linear relationships between age and power and phase-based connectivity, respectively. We also tested whether these trajectories differed between sexes, as males and females show divergent biological variations, for instance in brain volume (25, 26) and functional network connectivity (27). Some studies report sex differences in MEG (28-31) or EEG features (32-37) during or in absence of a task in various age ranges and frequencies. However, research efforts in this direction for the resting-state are generally limited. Another intriguing question is how lifetime changes in brain structure relate to functional outcomes. Cortical thickness is indicative of the brain's macrostructural organization and gradual thinning from childhood up into old age has been consistently reported, with a few exceptions for different age effects in the anterior cingulate cortex, entorhinal, and temporopolar cortices (38). A growing body of literature has established correlations between co-activation patterns and structural connectivity using MR imaging (39). However, the relation of haemodynamic connectivity during rest to MEG networks is complex and does not follow simple linear dynamics for single frequency bands (40, 41). Thus, we sought to extent the current perspective

on structure-function coupling and bring together lifespan patterns for the structural domain and fast neuronal activity measured using MRI and MEG.

Results

To probe adult lifespan differences in MEG markers we leveraged resting-state data from a sex-balanced subset of the Cambridge Centre for Aging and Neuroscience (Cam-CAN) project (n= 350), testing for linear and non-linear effects of age and interaction with sex. We then investigated age-related structural alterations in brains of the same individuals derived from anatomical MRI scans and spatial correspondence with age effects on connectivity and power. Finally, we explored if there is an overarching link between cortical structure and functional MEG levels when considering the entire lifespan data.

Lifespan differences in phase-based connectivity. We examined the relationship between age and MEG metrics at each of 2004 cortical surface points in the brain (vertices) for a local assessment and once averaged across the individual's brain to estimate global differences. Source projection of MEG signals was carried out in six conventional frequency bands (delta to gamma) and linear models were specified at each frequency band including age, age^2, sex, and total intracranial volume as independent variables. We pursued non-parametric testing by permutation analyses of the respective models (42).

We found that connectivity varied linearly with age in mainly posterior parts of the brain with similar topographies for the frequency bands studied, involving cuneus and inferior parietal regions ($p_{\mathrm{FWE}} < 0.05$). The direction of the effect was positive for the theta and gamma frequency bands and, conversely, negative in the alpha to high beta bands (**Figure 1**). Despite relatively local association patterns with age, the linear effects in these frequency bands were also significant on a global level for theta, alpha, and gamma (range global $r_{partial}$ = 0.09-0.17, **Suppl Table 2**). Interestingly, there was a different pattern for the low and high beta bands in central and frontotemporal regions that significantly followed a quadratic function with age **(Figure 1)**. That is, middle age groups exhibited the strongest beta connectivity levels in comparison with young or old age groups (vertex-wise and globally with $r_{partial}$ ranging from 0.18-0.21, **Suppl Table 2**). These findings suggest that differential maturation or aging processes in anterior-central regions compared with those in the occipital lobe are reflected in MEG connectivity. There was no evidence for significant interaction effects for age and sex, except for delta connectivity, such that females had a steeper slope for delta connectivity than males in the cuneus and parietal regions. At a global level, the interaction was not significant for the linear age effects, but for the quadratic age term, overall pointing to differences in delta connectivity between the sexes (**Figure 3, Suppl Table 4**).

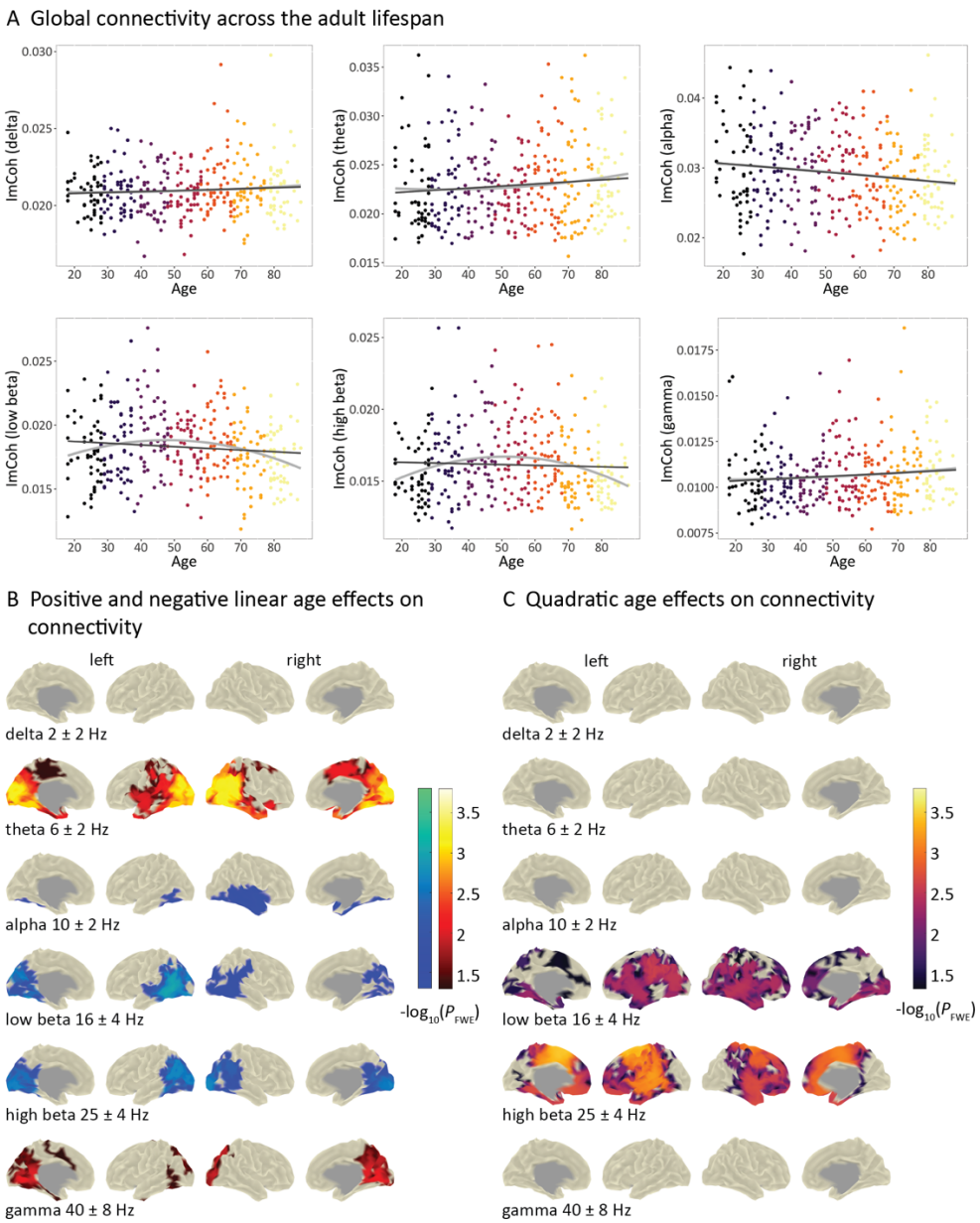

Figure 1. Frequency-specific associations between age and connectivity

(**A**) The plots show individual (raw) values of global connectivity ($n = 350$) across early and late adulthood for the six frequency bands investigated. The black lines represent linear relationships between age and global connectivity, while the gray lines represent quadratic relationships. Statistical analyses yielded significant linear effects of age in the theta, alpha, and gamma frequency bands. The quadratic term in the regression model was significant for the beta1 and beta2 bands. See **Suppl Table 2** for statistical details. In **(B)** and **(C)**, significant effects of age on vertex connectivity are highlighted. **(B)** The blue color bar indicates significant negative effects of age, whereas the red color bar represents significant positive associations. **(C)** The purple color bar indicates significant quadratic effects of age following an inverted U-shaped pattern (concave). Results for the U-shaped term (convex) were not significant and are not displayed. The significance level was set at -log10 $p > 1.3$ (equivalent to $p < 0.05$), family-wise error corrected (FWE). We estimated linear models for each frequency band separately with connectivity as the dependent variable, and age, age2, sex, and intracranial volume as independent variables and performed permutation-based analysis (at a global and vertex-level). ImCoh = imaginary part of coherency.

Lifespan differences in power. Collectively, the age effects on power were mostly distinct from those on connectivity and tended to be focused on anterior-temporal and central regions with shifts from lower to higher frequency bands. Specifically, power in the theta to gamma bands showed a significant positive association with age with most prominent effects in frontotemporal, insular, and central regions (**Figure 2**), and also globally in the beta to gamma frequencies (range global $r_{partial}$ = 0.11-0.25, **Suppl Table 3**). Furthermore, we observed quadratic age effects on power (**Figure 2**). Delta power and less strong theta power, globally showed a dip in the middle ages (range global $r_{partial}$ = 0.10-0.19, **Suppl Table 3**) with a strong anterior-basal emphasis, whereas the opposite direction was found for the beta and gamma bands peaking in the middle ages (range global $r_{partial}$ = 0.10-0.22). Of note, the quadratic age effects in high beta and gamma were prominent in the cingulate and central areas, overlapping spatially, at least in part, with the quadratic age effects on beta connectivity. As with connectivity, sex-specific analyses for power revealed differing lifespan trajectories for the delta band between males and females, with a stronger linear decline for men than women. This was the case in the global analysis **(Suppl Table 4)** as well as in frontocentral regions, cingulate, and precuneus **(Figure 3)**. In frontal brain areas, there was also an interaction effect between age and sex in the theta range, which was not significant at a global level (**Figure 3**; **Suppl Table 4**). Moreover, we found a significant main effect of sex in gamma power for a few clusters in the frontal cortex, but in absence of an interaction with age (data not shown).

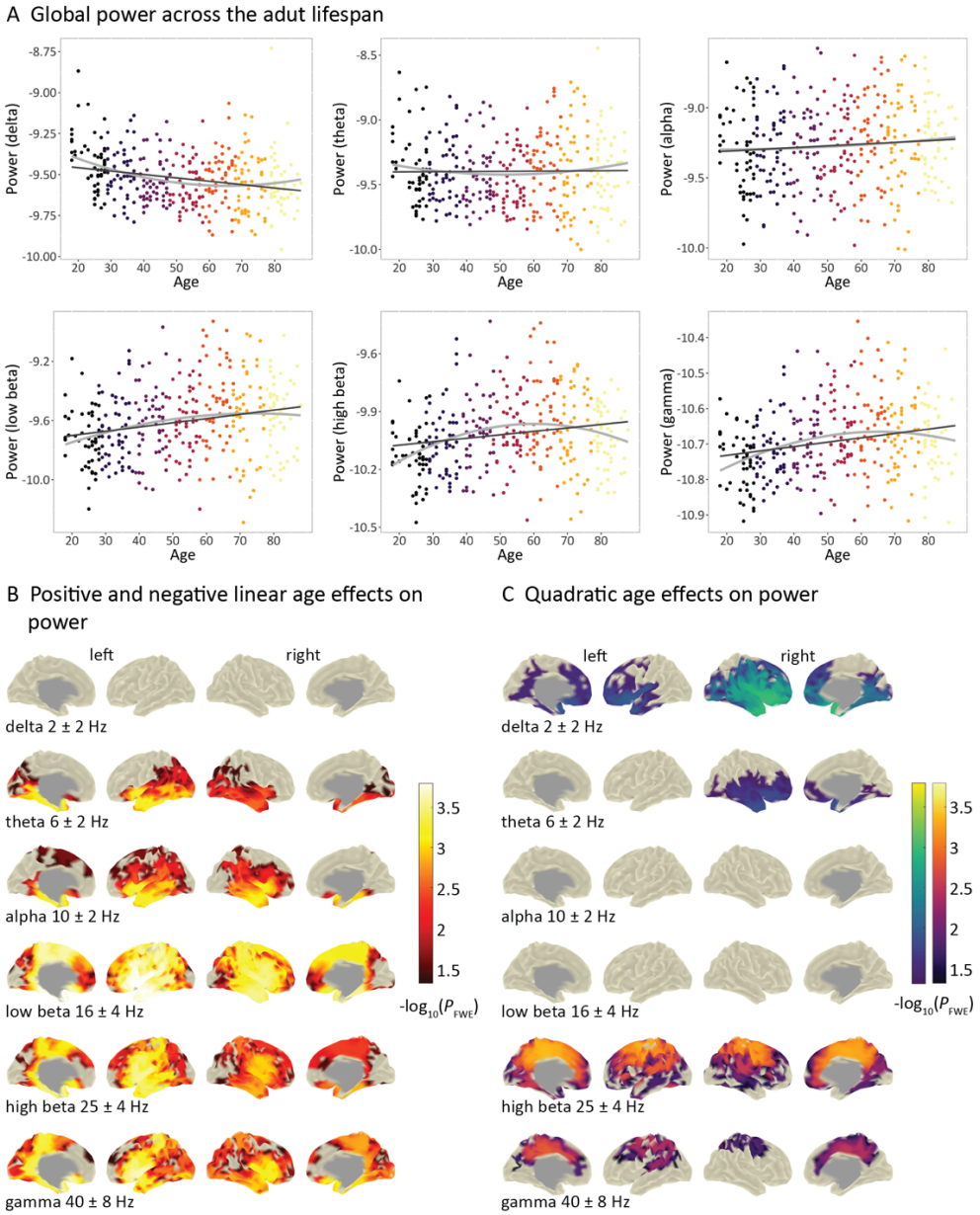

Figure 2. Frequency-specific associations between age and power

(**A**) The plots show individual (raw) values of global power (n = 350) across early and late adulthood for the six frequency bands investigated. The black lines represent linear relationships between age and global power, while the gray lines represent quadratic relationships. Power data was log10-transformed for visualization purposes. Statistical analyses yielded significant linear effects of age on global power in all frequency bands except for delta. The quadratic term in the regression model was significant for the delta, theta, beta1, beta2, and gamma bands. See **Suppl Table 3** for statistical details. In **(B)** and **(C)**, significant effects of age on vertex-power are highlighted. **(B)** The red color bar indicates significant positive effects of age. **(C)** The green color bar depicts significant quadratic effects of age following a U-shaped pattern (convex), while the purple color bar indicates significant effects following an inverted U (concave). The significance level was set at -log10 $p > 1.3$ (equivalent to $p < 0.05$), family-wise error corrected (FWE). We estimated linear models for each frequency band separately with power as the dependent variable, and age, age2, sex, and intracranial volume as independent variables and performed permutation-based analysis (at a global and vertex-level).

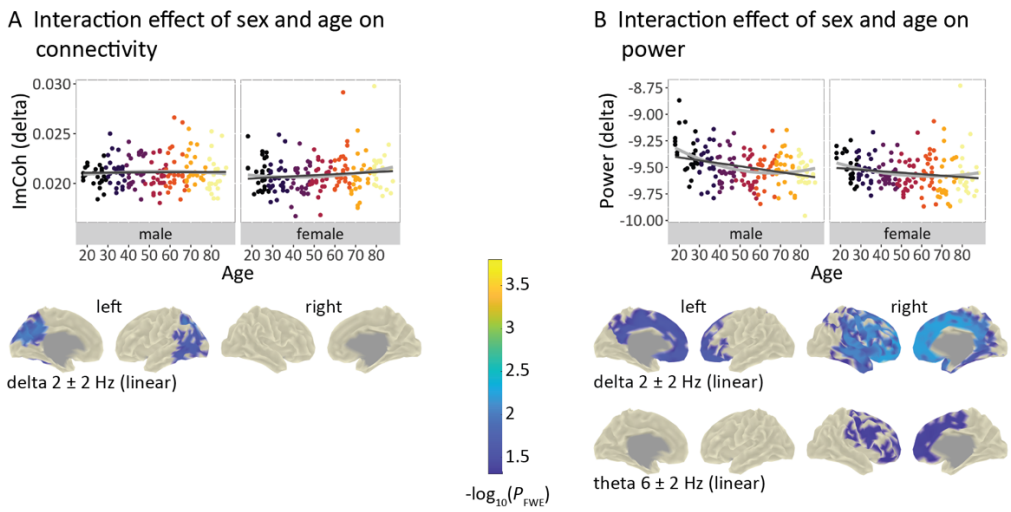

Figure 3. Sex-specific trajectories for MEG markers with age

(A) The plot shows individual global connectivity across early and late adulthood separately for males (n = 175) and females (n = 175) in the delta band, with a significant interaction of sex and age on global connectivity (quadratic effect), such that the age effect curve was narrower for females than for males. However, at the vertex-level, the slopes for the sexes were significantly different only for the linear age effect on delta connectivity and prominent in the cuneus. (B) Shown are significant interactions between sex and linear age effects on global power in the delta band and on delta and theta power at the vertex level, with emphasis on frontal regions. Global power data was log10-transformed for visualization purposes. The significance level was set at -log10 $p > 1.3$ (equivalent to $p < 0.05$), family-wise error corrected (FWE). We estimated linear models to test whether the age trajectories of power differed between males and females in each frequency band using permutation-based analysis. The black lines in the global plots represent linear relationships between age and global MEG values, while the gray lines represent quadratic relationships. See **Suppl Table 3 and 4** for statistical details.

Assessment of structural alterations across adulthood. To provide insights into how the brain's structural architecture interacts with fast oscillatory activity, we next investigated how cortical thickness varies across the adult lifespan. We analyzed individual cortical thickness based on 3T brain scans at each point of the cortical surface mesh and applied the same analysis principles for the mapping of age effects on the MEG markers. In accordance with previous reports (38), a dominant pattern of a significant gradual decrease of cortical thickness with age was observed. This linear age effect was significant, globally (p = 0.002) and in most of the brain areas investigated **(Figure 4A)**, particularly in temporal regions, supramarginal and inferior parietal regions, posterior cingulate, central, insular and caudle middle frontal regions. In a few regions, cortical thickness followed a quadratic trajectory with age, with the highest values in the middle age groups in the right temporal pole, parahippocampal and lateral occipital areas **(Figure 4A)**, as previously reported (38).

Relating lifespan patterns for cortical thickness and MEG markers. Next, we tested if age-related structural alterations spatially correspond to those on fast brain oscillations. We performed Spearman rank correlations between t-value maps of the age effects on cortical thickness (linear decrease, inverted-U-shape effect) and the age effects on connectivity and power, respectively. In each analysis, the correlation coefficient was tested against a spatially-

constrained null distribution generated using a spatial permutation model ("spin-test"; (43)) to preserve spatial autocorrelation of the maps. The cross-sectional course of cortical thickness mainly resembled the ones for beta and delta oscillations **(Figures 4B and 4C)**. Specifically, the linear decrease of cortical thickness with age was mostly correlated with age effects on MEG power, particularly in the beta (quadratic age effects low beta $r_s = .431$, $p_{spin} = 0.007$; high beta $r_s = .479$, $p_{spin} = 0.002$) and delta frequency bands (linear age effect, $r_s = .314$, $p_{spin} = 0.008$). This correspondence was weaker in the remaining frequency bands and did not reach significance after applying the spin test (r_s ranging from |.014-.366| for linear and quadratic age effects on power, $p_{spin} > 0.05$; **Suppl Table 5).** There was also a moderate, but significant correlation between cortical thinning and age effects on connectivity in the delta band (linear age effect, $r_s = .343$, $p_{spin} = 0.004$) and weaker, non-significant correlations in the remaining frequency bands (r_s ranging from |.051-.267| for linear and quadratic age effects, $p_{spin} > 0.05$; **Suppl Table 5**).

Conversely, patterns of quadratic age effects on cortical thickness mainly corresponded to age effects on connectivity, namely in the low beta band (linear age effect, $r_s = .360$, $p_{spin} = 0.024$), delta (quadratic age effect, $r_s = -.218$, $p_{spin} = 0.028$), and marginally in the alpha band (linear age effect, $r_s = .0.295$, $p_{spin} = 0.050$). There were no other significant overlaps between the t-statistics for cortical thickness and connectivity in the other frequency bands (r_s ranging from |<.001-.193| for linear and quadratic age effects, $p_{spin} > 0.05$; **Suppl Table 6**) nor with power maps (r_s ranging from |.012-.289| for linear and quadratic age effects, $p_{spin} > 0.05$; **Suppl Table 6**).

Correspondence of oscillatory activity and brain structure beyond age. To further assess the influence of brain structure on functional MEG markers, we estimated general linear models, including cortical thickness, age, age^2, sex, and total intracranial volume as independent variables across the whole study sample. We employed statistical permutation testing of the models (42), but at the level of functional resting-state networks, as described in Yeo*, et al.* (44), because strong structure-function correspondence can be expected in functionally relevant systems (45). With an exception for the delta band, there was a tendency of positive associations between cortical thickness and MEG levels in transmodal regions, and negative associations in unimodal regions (**Suppl Figure 2**). These were significant for connectivity in the slower frequency bands and power in the higher frequency bands (**Figure 4 D**). Specifically, delta connectivity in the ventral attention network was predicted by cortical thickness, which was also the case for the frontoparietal and motor networks when not corrected for the number of networks tested. Similarly, there was a positive association for theta and alpha connectivity in the DMN, but did not survive corrections for multiple comparisons. Conversely, cortical thickness in somatomotor and visual networks negatively predicted beta and gamma power in these regions. However, only the pattern for gamma power survived corrections.

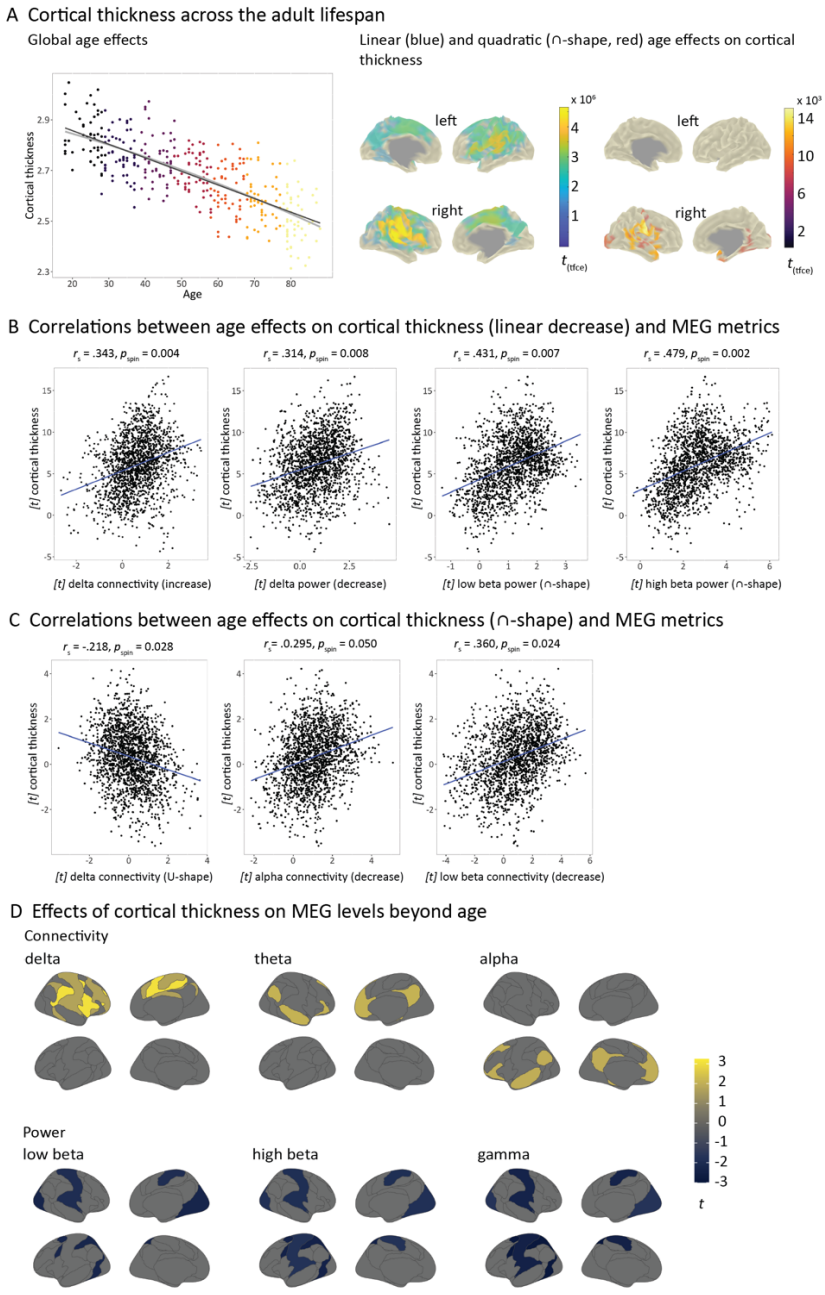

Figure 4. Age effects on cortical thickness and relation to MEG markers

(A) Age effects on global and vertex-wise cortical thickness across early and late adulthood. The black line represents the linear relationship between age and global thickness (p = 0.002), while the gray line represents a quadratic relationship (not significant). The linear negative age effect was significant in various brain regions with an emphasis on temporal-parietal regions (blue color bar). Cortical thickness in a few clusters followed a quadratic relationship with age (red color bar). Shown are t-values after threshold-free cluster enhancement (TFCE) for significant vertices. (B) The gradual decrease in cortical thickness significantly correlated with age-related patterns for mostly delta (linear) and beta power (quadratic), but also for delta connectivity (linear). (C) There was also a significant spatial overlap between the quadratic age effects on cortical thickness and those on delta (quadratic), alpha, and beta connectivity (linear). Spearman rank correlation coefficients (r_s) were tested for significance using a spatial permutation procedure (spin-test, 10.000 rotations). (D) Across the entire adult lifespan sample, cortical thickness levels significantly aligned with connectivity levels in the delta to alpha bands. A negative effect of cortical thickness was observed for high frequency power. Note that only the structure-function correspondence for delta connectivity in the ventral attention network and gamma power in the sensorimotor network survived corrections for the number of networks tested (FDR-correction).

Discussion

Using a large set of age-stratified MEG resting-state recordings, we provided insights into how phase-based connectivity and power are expressed in whole-brain networks from early adulthood to old age. The markers showed frequency-specific associations with age, likely reflecting physiological processes at various adult life stages. Phase coupling varied primarily in posterior brain regions in a linear fashion, whereas in central-temporal areas, beta band connectivity peaked at midlife. Remarkably, the direction of age effects on power differed in lower (delta/theta) and higher (> alpha) frequencies with foci in association and centrotemporal areas and the cingulate. Both sexes exhibited similar MEG trajectories except for delta/theta oscillations. The variability of cortical thickness with age mainly corresponded to that for delta and beta oscillations, suggesting that both modalities reflect similar maturation and aging processes. Across the entire study sample, cortical thickness predicted MEG levels in ventral attention and default mode networks (delta to alpha) and sensorimotor and visual networks (beta to gamma).

Local and distributed frequency-dependent connectivity differences with age. Very few studies have investigated phase-based neuronal organization across a broad age range (46) or used coherence as their connectivity measure (24), which is likely to be influenced by electromagnetic field spread. We employed the imaginary part of coherency, which has been reported to be less sensitive to this confound (47), and we incorporated other co-variables like sex and intracranial volume into our models. With respect to fMRI findings, shifts in functional activation patterns in the elderly have been attributed to functional compensatory mechanisms (48) or altered neuronal efficiency or specificity (49, 50). Remarkably, in our study, the linear age effects on phase coupling tended to be local and of similar topography, with the frequency bands possibly exhibiting different but related functional processes. Theta coupling appears to change along an anterior-posterior gradient with age, with frontal decreases during adolescence, which was related to cognitive control (19), and increases in posterior regions during adulthood (20), as observed in our analysis. In general, theta oscillations are believed to temporally coordinate higher-frequency activity, such as gamma (51), together supporting feedforward signaling in the visual cortex of primates (52). Feedback communication instead relied on the beta band (52). In our study, gamma connectivity also showed a similar age-dependent trend as in theta but differed from beta connectivity. In the Cam-CAN data set, the occurrence of microstates decreased with age in early visual areas (21, 53), potentially related to reduced selective responsiveness of the ventral visual cortex to visual stimuli and slowing of perceptual speed in the elderly (54). In higher-order brain areas, however, such transient neuronal states occurred more frequently with age, which correlated with lower fluid but not crystalline intelligence possibly indicating lower flexibility and coordination in the brain (53). We also found a different pattern for age effects in higher-order regions, compatible with the notion that these areas show protracted maturation compared with lower-order regions (13). Notably, this was only the case for connectivity in the beta band. Here, the levels peaked around the 50s, possibly subserving intellectual, behavioral, and socioemotional processes through distributed long-range connections in the brain (13, 55-57).

Age-related power shifts from low to high frequencies. Research on power alterations with age was undertaken early on covering different life decades (58), providing evidence for a shift from lower to higher frequency bands (19-21, 23, 59, 60). We add regional information for variability in power that was accentuated in insular and cingulate regions. Multiple, widely different functions in the brain are attributed to the insula, which is broadly connected to thalamic nuclei, limbic, and association areas (61). These include interoception that may vary gradually with age, for example, for pain, temperature, or tactile stimuli (62), as well as temporal and social perception (63). Besides linear age effects, we found U-shaped trajectories in anterior-basal areas for delta, and, to some extent, also for theta power, which might be linked to the development (64) or decline of frontal cognitive functions. For example, decline in executive functions with age is thought to be related to structural changes in the frontal lobe (65, 66). Consistently, a decrease in fluid intelligence and multitasking was found in the Cam-CAN data, to which specific prefrontal changes in gray and white matter contributed (67). Future studies should address this neurocognitive relationship across age in more detail, but the possible importance of delta oscillations for cognitive processes has been discussed previously (68). Power in higher frequency bands like high beta and gamma exhibited a reverse effect with midlife peaks in cingulate and central brain regions. Cingulate regions are considered part of the DMN (69), to change during aging (8), relate to internal cognition (69, 70), and have been proposed to contribute to metastability of intrinsic connectivity (71). Abnormal structure and function in this part of the cortex is associated with many neurological and psychiatric disorders with onset in adolescence and old age (72). One may speculate whether the non-linear power trajectories we found might commensurate with susceptibility for disease development at certain age windows. Our findings for the beta band in the central cortex might link to altered levels of event-related activity. Central regions and beta band activity are classically related to movement (73-75) and have been shown to change across the lifespan during button pressing tasks, as measured in the Cam-CAN data set (76). Altogether, power alterations in our study spatially encompassed the major players of the association and sensorimotor networks with different sensitivities for age effects. The reason for power shifts with age needs further investigation, as does a possible relationship between phase-connectivity and power in beta frequencies, whose trajectories exhibited some spatial overlap in our study.

Divergent MEG trajectories among adult males and females. Furthermore, our results point to sex-specific effects on resting-state variability in adults in low-frequency delta and theta after correcting for intracortical volume. So far, similar approaches using MEG in adults have been scarce. Our sample of 25 individuals of each sex per decade of life may not yet be sufficient to detect sex effects reliably. Also, lower reliability of M/EEG estimates in the delta range and susceptibility to noise might have led to the different slopes for males and females. On the other hand, our study was age- and sex-balanced and suggests differences in oscillations, which, as alluded to above, might play a dominant role in development and involution, tying in with earlier work. For example, a decline in slow-wave activity during adolescence is known from sleep research (64, 77), with boys exhibiting more delta power than girls during the course, indicating an earlier onset of changes in sleep homeostasis in girls (78). The "occipital delta of youth" is also a well-known EEG phenomenon that usually disappears with the transition to adulthood (79) and might follow a different course between the sexes, extending into middle and late adulthood. One study in adults reports sex-specific reconfigurations of EEG

microstates during maturation and in old age, similarly pointing to different trajectories of temporal dynamics for males and females (80). However, further studies should systematically focus on sex-dimorphic patterns using electrophysiology across adulthood and associate them with other phenotypes to explore behavioral associations.

Correspondence between MEG activity and cortical thickness across adulthood. Finally, we show that, at the cross-sectional level, the age trajectories for mainly delta and beta band oscillations spatially resembled that for cortical thickness. In general, the correspondence was of moderate effect size (r_s ~0.2-0.5), similar to previous attempts directly linking structural and functional connectivity using MRI (39). This seems plausible given that a mixture of brain rhythms can explain fMRI networks, but with a particular role for the beta band (40, 41). Notably, variation in cortical thickness is arranged along a poster-anterior axis that is thought to have unfolded during neurogenesis and to be related to myelination (13) and genetic components (81). Similarly, beta band power has been expressed closely along this principal axis, which was less stringent in the theta and alpha bands (82). This spatial co-variation of the modalities may also converge with findings of altered beta band signals and concomitant thickness patterns in genetic disorders (1, 83), as with comparably high heritability of MEG beta power in general (84). Moreover, evidence is accumulating that cortical alterations during development also occur along a hierarchical order (13), as mentioned previously, for example, for delta and beta power in opposite directions in an adolescent sample (19). Thus, it is conceivable that oscillatory activity and cortical macrostructure also follow spatially similar pathways during adulthood. Noteworthy, fMRI research in children and young adults suggests regional changes in structure-function coupling with age, preferentially for areas in the default mode (85, 86) and the ventral attention network (85). It has been proposed that these changes relate to functional and cognitive flexibility (86, 87). In our study of adults, cortical thickness significantly explained variance in MEG connectivity in these networks across the entire sample, hence across all age groups, and mainly in the delta to alpha frequencies. Interestingly, rapid state reconfigurations in these frequency bands have been shown to form the default mode activation pattern incorporating regions that support higher-order cognition (88). The coupling between cortical thickness and low-frequency neuromagnetic connectivity might thus be the backbone of cognitive processes during adulthood. Conversely, our data revealed a negative effect of cortical thickness on high-frequency power in sensorimotor, visual, and dorsal attention networks. The cortex in sensorimotor regions is thinner than in association areas and exhibits stronger myelination that has been related to beta and gamma activation patterns before (46), consistent with our findings. We further extend previous investigations on structure-function interrelations using MRI that have reported the opposite, that is, decoupling towards transmodal cortex but tight coupling in unimodal sensory and motor areas (39, 45). Therefore, the relationship between brain activity at different temporal scales and macro- and microstructural features may be non-trivial. Importantly, our results may rely on mixed effects or be driven by particular age groups and should be confirmed in appropriate samples with specific age ranges. In addition, simple correlative models may not be sufficiently suited to describe complex interactions between brain structure and function. As previously suggested, microscale attributes and detailed topological information could substantially improve the modeling approaches (39).

Further considerations. Important limitations should be kept in mind. First, our study results are based on selected MEG signal characteristics averaged across the time domain rather than time-resolved dynamics. Second, the relatively small effect sizes of the age effects on the global estimates suggest that many other factors contribute to the variance in our data. And third, the cross-sectional design of the study is not suitable for determining individual long-term trajectories (89) and cohort effects cannot be excluded (90). Nonetheless, our results have important implications for a number of studies using M/EEG. When applying similar measures in clinical cohorts, convergence or divergence from the patterns in healthy individuals could be tested, primarily to understand brain pathology but also to advance the development of biological disease markers.

Conclusion. Overall, we complement age-related (f)MRI literature with investigations of fast neuronal activity at rest. We show that MEG characteristics vary considerably during adulthood with frequency- and sex-specific trajectories. Age effects on connectivity were present along the cortical hierarchy, linearly in lower-order visual areas and with beta band peaks at midlife in motor and association regions. Gradual age patterns for power were prominent in brain regions associated with interoception. Power dips and peaks at midlife were observed for low frequencies in the frontal lobe versus high frequencies in central and cingulate areas, often affected in pathological states. Cortical thickness showed similar aging patterns as delta and beta oscillations and a close relationship with neuromagnetic activity in the default mode, attention, and motor networks.

Materials and Methods

Data and participants. In our study, we used cross-sectional open-access data provided by the Cambridge Centre for Aging and Neuroscience (Cam-CAN) data repository. The Cam-CAN project encompassed several phases, including cognitive assessments, interviews and health and lifestyle questionnaires, and structural and functional brain examinations (91). Approximately 650 resting-state MEG data sets and anatomical scans were available from phase two of the study (92), a subset of which we initially analyzed (n = 450). After excluding data with motion artifacts, noise, sleep, or failed Freesurfer reconstruction (n_{excluded} = 72), 350 cleaned MEG and MRI data were randomly selected from the remaining data sets for further analysis in a balanced design. In total, we report on seven age groups, each with 50 individuals aged 18 to 88 years, divided into ten-year increments and balanced by sex (see demographic data in **Table 1**). All included individuals were cognitively normal (Mini Mental State Examination score < 24; Folstein, Folstein and McHugh (93)) and free of neurological or psychiatric conditions (e.g. dementia, epilepsy, head injury with severe sequelae, bipolar disorder, schizophrenia) and substance abuse history. Individuals with communication problems (hearing, speech, or visual impairment), limited mobility, or MRI/MEG contraindications were excluded. For details on the study protocol and datasets see Shafto*, et al.* (91). The study was conducted in accordance with the Declaration of Helsinki (94) and approved by the local ethics committee, Cambridgeshire 2 Research Ethics Committee. Data collection and sharing for this project was provided by the Cam-CAN.

MRI acquisition. Anatomical data were acquired using a 3T Siemens TIM Trio scanner with a 32-channel head coil. T1-weighted images were derived from 3D MPRAGE sequences with TR=2250ms, TE=2.99ms, TI=900ms; FA=9 deg; FOV=256x240x192mm; 1mm isotropic; GRAPPA=2; TA=4mins 32s), and T2-weighted images from 3D SPACE sequences with TR=2800ms, TE=408ms, TI=900ms; FOV=256x256x192mm; 1mm isotropic; GRAPPA=2; TA=4mins 30s).

MEG acquisition. Resting-state data were recorded using a 306-channel VectorView MEG system (Elekta Neuromag, Helsinki) with 102 magnetometers and 204 planar gradiometers (sampling at 1 kHz with a 0.03 Hz high pass filter). Individuals were assessed in a seated position in a magnetically shielded room at a single site (MRC Cognition and Brain Science Unit, University of Cambridge, UK) for 8 min and 40 s. At the same time, four coils continuously measured the head position within the MEG helmet. Additionally, electrocardiogram (ECG) and electrooculogram (horizontal and vertical) were recorded to track cardiac signals and eye-movements. Individuals were instructed to keep their eyes closed and sit still.

MRI processing and individual head models. For mapping MEG sensor level data onto individual cortical surfaces, anatomical information was derived from T1- and T2-weighted images and reconstructed using FreeSurfer 6.0.0 (https://surfer.nmr.mgh.harvard.edu/). We applied surface-based mapping (SUMA (95)), which resampled the cortical surfaces to 1,002 vertices per hemisphere (ld factor = 10), based on the 'fsaverage' template mesh provided by FreeSurfer and SUMA. The individual meshes were realigned to the Neuromag sensor space based on anatomical landmark coordinates provided by Cam-CAN. We used the "single shell" method implemented in Fieldtrip to compute the leadfields and individual head models for MEG source projection.

MEG processing. Preprocessed MEG data was available through the Cam-CAN repository. For each dataset Elekta Neuromag Maxfilter 2.2 was applied using temporal signal space separation (10s window, 0.98 correlation limit) to remove external interference and artefacts, line noise (50 Hz and its harmonics), and to correct for bad channels and head movements. Using Fieldtrip (96), we resampled the data to 300 Hz, initially high-pass filtered at 1 Hz (first order Butterworth), and segmented the data into trials of 10 s length. Trials containing artifacts were removed following an automatic approach for both MEG channel types separately (see https://www.fieldtriptoolbox.org/tutorial/automatic_artifact_rejection/ for further details). In brief, the data was bandpass filtered at 110 to 140 Hz (9th order Butterworth) for optimal detection of muscle artifacts and z-transformed for each channel and timepoint. The z-transformed values were averaged over all channels so that artifacts accumulated and could be detected in a time course representing standardized deviations from the mean of all channels. Finally, all time points that belonged to the artifact were marked using artifact padding, and data trials whose z-values were above a threshold of 14 were excluded. The remaining data were then low-pass filtered at 70 Hz (first-order Butterworth), and independent component analysis (ICA) was applied. Ocular components were automatically identified based on their similarity to EOG channel signals (average coherence > 0.3 and amplitude correlation coefficient > 0.4). Cardiac components were identified when coherent with the ECG signal

(average coherence > 0.3) or based on the averaged maximum peaks timelocked to the ECG (QRS complex, see https://www.fieldtriptoolbox.org/example/use_independent_component_analysis_ica_to_remove_ecg_artifacts/). For each data set, the automatic selection of the components was visually checked. In a few cases, we had to manually select the relevant ICA components because the ECG/EOG was noisy. We visually inspected all cleaned data for quality control and rated vigilance of individuals according to the criteria of the American Academy of Sleep Medicine (https://aasm.org/). Thirty trials from the cleaned data scored as "awake" were randomly selected for source analysis using signals from magnetometers (102 channels) only. We used beamforming (dynamic imaging of coherent sources (97)) to project sensor data to the surface points (source space) in the frequency domain. MEG power and cross-spectral densities were computed for six conventional frequency bands (delta: 2 ± 2 Hz, theta: 6 ± 2 Hz, alpha 10 ± 2 Hz, beta1 16 ± 4 Hz, beta2 25 ± 4 Hz and gamma 40 ± 8 Hz) based on fast Fourier spectral analysis using multitapers (Discrete Prolate Spheroidal Sequences tapers). Source projection was carried out using leadfields and adaptive spatial filters (regularization: lambda = 5%). The coherency coefficient was estimated between all pairs of vertices (source points, $n = 2238$) and the imaginary part was derived to account for potential field spread (47). The absolute imaginary part of coherency was our connectivity measure of interest, reflecting phase synchrony between signals. We averaged all connections of a vertex to obtain the overall strength of a vertex, and for each individual also across all vertices to get a global connectivity and power index. To provide an overview of connectivity and power distributions across the age groups, the frequency spectra of each individual in this study were calculated for 1-Hz bins and averaged for each age group (**Suppl Figure 1**).

Cortical thickness estimations. At each vertex of the cortical surface derived from the Freesurfer/SUMA procedure, individual cortical thickness measures were calculated, which describe the distance between the gray-white matter and pial boundaries. Smoothing of individual thickness maps were applied using a heat kernel of size 12 mm full width at half maximum in AFNI (https://afni.nimh.nih.gov/).

Permutation-based analysis of lifespan differences and structure-function relationships. We examined the relationship between age and the imaging metrics (connectivity, power, or cortical thickness) by fitting linear models with the metrics as dependent variables and age, age^2, sex, and intracranial volume as independent variables. We centered the individual age values before squaring them to reduce the correlation between the linear and the quadratic terms. The models were estimated either for the global metrics or for the metrics at each vertex (surface point) in the brain. The non-parametric statistic tool PALM (Permutation Analysis of Linear Models, (42)) was used to generate permutations for the respective models with tail approximation for accelerated inference (500 permutations) (98). Single t contrasts were computed, that is, for positive and negative linear age effects, and for convex and concave quadratic age terms. Using PALM, we also investigated sex differences in the trajectory of connectivity and power over the lifespan. For each age decade, 25 males and 25 females were included to ensure a balanced design giving 175 individuals per sex in total. Models were fitted to test whether the beta coefficients for the age and age^2 effects on connectivity or power in each frequency band differed between males and females while correcting for the influence of

total intracranial volume. For all analyses using the above described permutation approach, *p*-values were derived from the permutation distribution, at the tail of which a generalized Pareto distribution was fitted (98), and corrected for multiple comparisons (family-wise error, FWE) at cluster level resulting from threshold-free cluster enhancement (99). We set the significance level at $p = 0.05$ or equivalently $-\log10(p) \sim 1.3$. The partial correlation coefficient ($r_{partial}$) was estimated as an effect size for the independent variables based on the *t*-values and degrees of freedom of the global models (100). $r_{partial}$ indicates the degree of association between two variables at which the influence of other variables in the model has been eliminated (101): values of ± 0.1 reflect a small effect, ± 0.3 represent a moderate effect, and ± 0.5 is a large effect (102).

To examine the correlation between MEG markers and cortical thickness across the lifespan sample, we averaged the individual values across vertices corresponding to respective functional resting-state networks (44). PALM was run for each of the networks on both hemispheres and false discovery rate (FDR) applied to correct for multiple comparisons at the 14 networks. For each network, we report the effect of cortical thickness on the MEG markers after correcting for the effects of age, age^2, sex, and total intracranial volume.

Spin-tests for correspondence of age effects on brain structure and MEG markers. To statistically relate age effects on connectivity or power to those on cortical thickness, we used the unthresholded t-value maps derived from the main analyses on lifespan differences without the application of threshold-free cluster enhancement (99). We estimated Spearman rank correlations between the t-maps for the linear (negative) and quadratic (inverted U-shaped) age effects on cortical thickness and the maps of the linear and quadratic age effects on connectivity and power, respectively. Statistical significance for each correlation was assessed based on null distributions generated using 10,000 random rotations of the spherical projection of the cortical surface (SUMA) ("spin-test" (43)). This approach ensures the spatial embeddedness of the t-maps, as the rotational alignment is randomized rather than assuming exchangeability of the surface points. Rotations were applied to each hemisphere separately. The significance level was set to 5%.

Data availability

Raw data were provided by the Cam-CAN project and are available at https://camcan-archive.mrc-cbu.cam.ac.uk/dataaccess/ under specified conditions. Main processed MEG and structural data and all code used for the pre-processing, statistical analyses, and visualization of the results have been deposited in https://github.com/chstier/Lifespan_MEG.

Acknowledgments

Data collection and sharing for this project was provided by the Cambridge Centre for Ageing and Neuroscience (CamCAN). Cam-CAN funding was provided by the UK Biotechnology and Biological Sciences Research Council (grant number BB/H008217/1), together with support from the UK Medical Research Council and University of Cambridge, UK. This work was

further supported by the German Research Foundation (DFG; grant number FO 750/5-1 to N.K.F.)

Disclosure

N.K. Focke has received speaker bureau and consultancy fees from Arvelle/Angelini, Bial, and Eisai, all unrelated to the present project. C. Stier and C. Braun have no relevant financial or non-financial interests to disclose.

References

1. C. Stier *et al.*, Heritability of magnetoencephalography phenotypes among patients with genetic generalized epilepsy and their siblings. *Neurology* **97**, e166-e177 (2021).
2. Y. L. Hegner *et al.*, Increased functional MEG connectivity as a hallmark of MRI-negative focal and generalized epilepsy. *Brain topography* **31**, 863-874 (2018).
3. A. Elshahabi *et al.*, Magnetoencephalography reveals a widespread increase in network connectivity in idiopathic/genetic generalized epilepsy. *PLoS One* **10**, e0138119 (2015).
4. J. Hirvonen *et al.*, Whole-brain source-reconstructed MEG-data reveal reduced long-range synchronization in chronic schizophrenia. *ENeuro* **4** (2017).
5. R. Kurimoto *et al.*, Event-related synchronization of alpha activity in early Alzheimer's disease and mild cognitive impairment: an MEG study combining beamformer and group comparison. *Neuroscience letters* **443**, 86-89 (2008).
6. C. J. Stam *et al.*, Generalized synchronization of MEG recordings in Alzheimer's disease: evidence for involvement of the gamma band. *Journal of Clinical Neurophysiology* **19**, 562-574 (2002).
7. S. Oldham, G. Ball, A. Fornito, Early and late development of hub connectivity in the human brain. *Current opinion in psychology* **44**, 321-329 (2022).
8. J. S. Damoiseaux, Effects of aging on functional and structural brain connectivity. *Neuroimage* **160**, 32-40 (2017).
9. L. K. Ferreira, G. F. Busatto, Resting-state functional connectivity in normal brain aging. *Neuroscience & Biobehavioral Reviews* **37**, 384-400 (2013).
10. S. M. Grieve, C. R. Clark, L. M. Williams, A. J. Peduto, E. Gordon, Preservation of limbic and paralimbic structures in aging. *Human brain mapping* **25**, 391-401 (2005).
11. G. Kalpouzos *et al.*, Voxel-based mapping of brain gray matter volume and glucose metabolism profiles in normal aging. *Neurobiology of aging* **30**, 112-124 (2009).
12. D. Terribilli *et al.*, Age-related gray matter volume changes in the brain during non-elderly adulthood. *Neurobiology of aging* **32**, 354-368 (2011).
13. V. J. Sydnor *et al.*, Neurodevelopment of the association cortices: Patterns, mechanisms, and implications for psychopathology. *Neuron* **109**, 2820-2846 (2021).
14. K. Onoda, M. Ishihara, S. Yamaguchi, Decreased functional connectivity by aging is associated with cognitive decline. *Journal of cognitive neuroscience* **24**, 2186-2198 (2012).
15. D. Tomasi, N. D. Volkow, Aging and functional brain networks. *Molecular psychiatry* **17**, 549-558 (2012).
16. C. C. Huang *et al.*, Age-related changes in resting-state networks of a large sample size of healthy elderly. *CNS Neuroscience & Therapeutics* **21**, 817-825 (2015).

17. K. A. Tsvetanov *et al.*, The effect of ageing on f MRI: Correction for the confounding effects of vascular reactivity evaluated by joint f MRI and MEG in 335 adults. *Human brain mapping* **36**, 2248-2269 (2015).
18. S. Sadaghiani, M. J. Brookes, S. Baillet, Connectomics of human electrophysiology. *NeuroImage* **247**, 118788 (2022).
19. S. Marek *et al.*, Adolescent development of cortical oscillations: Power, phase, and support of cognitive maturation. *PLoS biology* **16**, e2004188 (2018).
20. B. A. Hunt *et al.*, Spatial and spectral trajectories in typical neurodevelopment from childhood to middle age. *Network Neuroscience* **3**, 497-520 (2019).
21. N. Coquelet *et al.*, Changes in electrophysiological static and dynamic human brain functional architecture from childhood to late adulthood. *Scientific Reports* **10**, 1-14 (2020).
22. C. B. Schäfer, B. R. Morgan, A. X. Ye, M. J. Taylor, S. M. Doesburg, Oscillations, networks, and their development: MEG connectivity changes with age. *Human brain mapping* **35**, 5249-5261 (2014).
23. C. Gómez, J. M. Perez-Macias, J. Poza, A. Fernández, R. Hornero, Spectral changes in spontaneous MEG activity across the lifespan. *Journal of neural engineering* **10**, 066006 (2013).
24. B. Sahoo, A. Pathak, G. Deco, A. Banerjee, D. Roy, Lifespan associated global patterns of coherent neural communication. *Neuroimage* **216**, 116824 (2020).
25. A. N. Ruigrok *et al.*, A meta-analysis of sex differences in human brain structure. *Neuroscience & Biobehavioral Reviews* **39**, 34-50 (2014).
26. S. J. Ritchie *et al.*, Sex differences in the adult human brain: evidence from 5216 UK biobank participants. *Cerebral cortex* **28**, 2959-2975 (2018).
27. T. D. Satterthwaite *et al.*, Linked sex differences in cognition and functional connectivity in youth. *Cerebral cortex* **25**, 2383-2394 (2015).
28. H. Hoshi, Y. Shigihara, Age-and gender-specific characteristics of the resting-state brain activity: a magnetoencephalography study. *Aging (Albany NY)* **12**, 21613 (2020).
29. B. K. Taylor *et al.*, Neural oscillatory dynamics serving abstract reasoning reveal robust sex differences in typically-developing children and adolescents. *Developmental Cognitive Neuroscience* **42**, 100770 (2020).
30. M. Azanova, M. H. Ruiz, A. V. Belianin, V. Klucharev, V. V. Nikulin, Resting-state theta oscillations and reward sensitivity in risk taking. *Frontiers in neuroscience* **15** (2021).
31. M. H. Fung *et al.*, Sexually dimorphic development in the cortical oscillatory dynamics serving early visual processing. *Developmental Cognitive Neuroscience*, 100968 (2021).
32. D. J. Smit, C. J. Stam, D. Posthuma, D. I. Boomsma, E. J. De Geus, Heritability of "small-world" networks in the brain: A graph theoretical analysis of resting-state EEG functional connectivity. *Human brain mapping* **29**, 1368-1378 (2008).
33. S. E. Kober, C. Neuper, Sex differences in human EEG theta oscillations during spatial navigation in virtual reality. *International Journal of Psychophysiology* **79**, 347-355 (2011).
34. R. P. Brenner, R. F. Ulrich, C. F. Reynolds III, EEG spectral findings in healthy, elderly men and women—sex differences. *Electroencephalography and clinical neurophysiology* **94**, 1-5 (1995).
35. M. Thordstein, N. Löfgren, A. Flisberg, K. Lindecrantz, I. Kjellmer, Sex differences in electrocortical activity in human neonates. *Neuroreport* **17**, 1165-1168 (2006).
36. A. R. Clarke, R. J. Barry, R. McCarthy, M. Selikowitz, Age and sex effects in the EEG: development of the normal child. *Clinical neurophysiology* **112**, 806-814 (2001).

37. R. J. Davidson, G. E. Schwartz, E. Pugash, E. Bromfield, Sex differences in patterns of EEG asymmetry. *Biological Psychology* **4**, 119-137 (1976).
38. S. Frangou *et al.*, Cortical thickness across the lifespan: Data from 17,075 healthy individuals aged 3–90 years. *Human brain mapping* **43**, 431-451 (2022).
39. L. E. Suárez, R. D. Markello, R. F. Betzel, B. Misic, Linking structure and function in macroscale brain networks. *Trends in Cognitive Sciences* **24**, 302-315 (2020).
40. P. Tewarie *et al.*, Predicting haemodynamic networks using electrophysiology: The role of non-linear and cross-frequency interactions. *Neuroimage* **130**, 273-292 (2016).
41. G. Shafiei, S. Baillet, B. Misic, Human electromagnetic and haemodynamic networks systematically converge in unimodal cortex and diverge in transmodal cortex. *PLoS biology* **20**, e3001735 (2022).
42. A. M. Winkler, G. R. Ridgway, M. A. Webster, S. M. Smith, T. E. Nichols, Permutation inference for the general linear model. *Neuroimage* **92**, 381-397 (2014).
43. A. F. Alexander-Bloch *et al.*, On testing for spatial correspondence between maps of human brain structure and function. *Neuroimage* **178**, 540-551 (2018).
44. B. T. Yeo *et al.*, The organization of the human cerebral cortex estimated by intrinsic functional connectivity. *Journal of neurophysiology* (2011).
45. B. Vázquez-Rodríguez *et al.*, Gradients of structure–function tethering across neocortex. *Proceedings of the National Academy of Sciences* **116**, 21219-21227 (2019).
46. B. A. Hunt *et al.*, Relationships between cortical myeloarchitecture and electrophysiological networks. *Proceedings of the National Academy of Sciences* **113**, 13510-13515 (2016).
47. G. Nolte *et al.*, Identifying true brain interaction from EEG data using the imaginary part of coherency. *Clinical neurophysiology* **115**, 2292-2307 (2004).
48. S. W. Davis, N. A. Dennis, S. M. Daselaar, M. S. Fleck, R. Cabeza, Que PASA? The posterior–anterior shift in aging. *Cerebral cortex* **18**, 1201-1209 (2008).
49. L. Nyberg, M. Lövdén, K. Riklund, U. Lindenberger, L. Bäckman, Memory aging and brain maintenance. *Trends in cognitive sciences* **16**, 292-305 (2012).
50. A. M. Morcom, R. N. Henson, Increased prefrontal activity with aging reflects nonspecific neural responses rather than compensation. *Journal of Neuroscience* **38**, 7303-7313 (2018).
51. R. T. Canolty *et al.*, High gamma power is phase-locked to theta oscillations in human neocortex. *science* **313**, 1626-1628 (2006).
52. A. M. Bastos *et al.*, Visual areas exert feedforward and feedback influences through distinct frequency channels. *Neuron* **85**, 390-401 (2015).
53. R. Tibon *et al.*, Transient neural network dynamics in cognitive ageing. *Neurobiology of Aging* **105**, 217-228 (2021).
54. D. C. Park *et al.*, Aging reduces neural specialization in ventral visual cortex. *Proceedings of the National Academy of Sciences* **101**, 13091-13095 (2004).
55. N. Kopell, G. Ermentrout, M. Whittington, R. Traub, Gamma rhythms and beta rhythms have different synchronization properties. *Proceedings of the National Academy of Sciences* **97**, 1867-1872 (2000).
56. R. L. Buckner, F. M. Krienen, The evolution of distributed association networks in the human brain. *Trends in cognitive sciences* **17**, 648-665 (2013).
57. J. Sepulcre *et al.*, The organization of local and distant functional connectivity in the human brain. *PLoS computational biology* **6**, e1000808 (2010).
58. F. H. Duffy, M. S. Albert, G. McAnulty, A. J. Garvey, Age-related differences in brain electrical activity of healthy subjects. *Annals of Neurology: Official Journal of the American Neurological Association and the Child Neurology Society* **16**, 430-438 (1984).

59. K. J. Whitaker *et al.*, Adolescence is associated with genomically patterned consolidation of the hubs of the human brain connectome. *Proceedings of the National Academy of Sciences* **113**, 9105-9110 (2016).
60. V. Miskovic *et al.*, Developmental changes in spontaneous electrocortical activity and network organization from early to late childhood. *Neuroimage* **118**, 237-247 (2015).
61. R. Nieuwenhuys, The insular cortex: a review. *Progress in brain research* **195**, 123-163 (2012).
62. C. L. Jones, J. Ward, H. D. Critchley, The neuropsychological impact of insular cortex lesions. *Journal of Neurology, Neurosurgery & Psychiatry* **81**, 611-618 (2010).
63. A. Schirmer, W. H. Meck, T. B. Penney, The socio-temporal brain: Connecting people in time. *Trends in cognitive sciences* **20**, 760-772 (2016).
64. I. G. Campbell, I. Feinberg, Longitudinal trajectories of non-rapid eye movement delta and theta EEG as indicators of adolescent brain maturation. *Proceedings of the National Academy of Sciences* **106**, 5177-5180 (2009).
65. P. M. Greenwood, The frontal aging hypothesis evaluated. *Journal of the International Neuropsychological Society* **6**, 705-726 (2000).
66. R. West, In defense of the frontal lobe hypothesis of cognitive aging. *Journal of the International Neuropsychological Society* **6**, 727-729 (2000).
67. R. A. Kievit *et al.*, Distinct aspects of frontal lobe structure mediate age-related differences in fluid intelligence and multitasking. *Nature communications* **5**, 1-10 (2014).
68. T. Harmony, The functional significance of delta oscillations in cognitive processing. *Frontiers in integrative neuroscience* **7**, 83 (2013).
69. R. L. Buckner, J. R. Andrews-Hanna, D. L. Schacter, The brain's default network: anatomy, function, and relevance to disease. *Annals of the new York Academy of Sciences* **1124**, 1-38 (2008).
70. M. E. Raichle *et al.*, A default mode of brain function. *Proceedings of the National Academy of Sciences* **98**, 676-682 (2001).
71. R. Leech, D. J. Sharp, The role of the posterior cingulate cortex in cognition and disease. *Brain* **137**, 12-32 (2014).
72. D. Zhang, M. E. Raichle, Disease and the brain's dark energy. *Nature Reviews Neurology* **6**, 15-28 (2010).
73. G. Pfurtscheller, C. Neuper, Motor imagery activates primary sensorimotor area in humans. *Neuroscience letters* **239**, 65-68 (1997).
74. G. Pfurtscheller, A. Stancak Jr, C. Neuper, Post-movement beta synchronization. A correlate of an idling motor area? *Electroencephalography and clinical neurophysiology* **98**, 281-293 (1996).
75. M. T. Jurkiewicz, W. C. Gaetz, A. C. Bostan, D. Cheyne, Post-movement beta rebound is generated in motor cortex: evidence from neuromagnetic recordings. *Neuroimage* **32**, 1281-1289 (2006).
76. T. Bardouille, L. Bailey, C. Group, Evidence for age-related changes in sensorimotor neuromagnetic responses during cued button pressing in a large open-access dataset. *NeuroImage* **193**, 25-34 (2019).
77. I. G. Campbell *et al.*, Adolescent changes in homeostatic regulation of EEG activity in the delta and theta frequency bands during NREM sleep. *Sleep* **34**, 83-91 (2011).
78. I. G. Campbell, N. Darchia, W. Y. Khaw, L. M. Higgins, I. Feinberg, Sleep EEG evidence of sex differences in adolescent brain maturation. *Sleep* **28**, 637-643 (2005).
79. A. Ebner, G. Deuschl, T. Bast (2006) EEG. RRN-Referenz-Reihe Neurologie-Methoden. (Thieme, Stuttgart).

80. M. Tomescu *et al.*, From swing to cane: sex differences of EEG resting-state temporal patterns during maturation and aging. *Developmental cognitive neuroscience* **31**, 58-66 (2018).
81. S. L. Valk *et al.*, Shaping brain structure: Genetic and phylogenetic axes of macroscale organization of cortical thickness. *Science Advances* **6**, eabb3417 (2020).
82. K. Mahjoory, J.-M. Schoffelen, A. Keitel, J. Gross, The frequency gradient of human resting-state brain oscillations follows cortical hierarchies. *Elife* **9**, e53715 (2020).
83. C. Stier *et al.*, Combined electrophysiological and morphological phenotypes in patients with genetic generalized epilepsy and their healthy siblings. *Epilepsia* **63**, 1643-1657 (2022).
84. G. L. Colclough *et al.*, The heritability of multi-modal connectivity in human brain activity. *Elife* **6**, e20178 (2017).
85. B.-y. Park *et al.*, Adolescent development of multiscale structural wiring and functional interactions in the human connectome. *Proceedings of the National Academy of Sciences* **119**, e2116673119 (2022).
86. G. L. Baum *et al.*, Development of structure–function coupling in human brain networks during youth. *Proceedings of the National Academy of Sciences* **117**, 771-778 (2020).
87. J. D. Medaglia *et al.*, Functional alignment with anatomical networks is associated with cognitive flexibility. *Nature human behaviour* **2**, 156-164 (2018).
88. D. Vidaurre *et al.*, Spontaneous cortical activity transiently organises into frequency specific phase-coupling networks. *Nature communications* **9**, 1-13 (2018).
89. U. Lindenberger, T. Von Oertzen, P. Ghisletta, C. Hertzog, Cross-sectional age variance extraction: what's change got to do with it? *Psychology and aging* **26**, 34 (2011).
90. M. Sliwinski, L. Hoffman, S. M. Hofer, Evaluating convergence of within-person change and between-person age differences in age-heterogeneous longitudinal studies. *Research in Human Development* **7**, 45-60 (2010).
91. M. A. Shafto *et al.*, The Cambridge Centre for Ageing and Neuroscience (Cam-CAN) study protocol: a cross-sectional, lifespan, multidisciplinary examination of healthy cognitive ageing. *BMC neurology* **14**, 1-25 (2014).
92. J. R. Taylor *et al.*, The Cambridge Centre for Ageing and Neuroscience (Cam-CAN) data repository: Structural and functional MRI, MEG, and cognitive data from a cross-sectional adult lifespan sample. *Neuroimage* **144**, 262-269 (2017).
93. M. F. Folstein, S. E. Folstein, P. R. McHugh, "Mini-mental state": a practical method for grading the cognitive state of patients for the clinician. *Journal of psychiatric research* **12**, 189-198 (1975).
94. World Medical Association, World Medical Association Declaration of Helsinki: Ethical Principles for Medical Research Involving Human Subjects. *JAMA* **310**, 2191-2194 (2013).
95. Z. S. Saad, R. C. Reynolds, Suma. *Neuroimage* **62**, 768-773 (2012).
96. R. Oostenveld, P. Fries, E. Maris, J.-M. Schoffelen, FieldTrip: open source software for advanced analysis of MEG, EEG, and invasive electrophysiological data. *Computational intelligence and neuroscience* **2011** (2011).
97. J. Gross *et al.*, Dynamic imaging of coherent sources: studying neural interactions in the human brain. *Proceedings of the National Academy of Sciences* **98**, 694-699 (2001).
98. A. M. Winkler, G. R. Ridgway, G. Douaud, T. E. Nichols, S. M. Smith, Faster permutation inference in brain imaging. *Neuroimage* **141**, 502-516 (2016).
99. S. M. Smith, T. E. Nichols, Threshold-free cluster enhancement: addressing problems of smoothing, threshold dependence and localisation in cluster inference. *Neuroimage* **44**, 83-98 (2009).
100. R. Rosenthal, H. Cooper, L. Hedges, Parametric measures of effect size. *The handbook of research synthesis* **621**, 231-244 (1994).

101. J. Bortz, C. Schuster, *Statistik für Human-und Sozialwissenschaftler: Limitierte Sonderausgabe* (Springer-Verlag, 2011).
102. A. Field, J. Miles, Z. Field (2012) Discovering statistics using R. (Sage London).

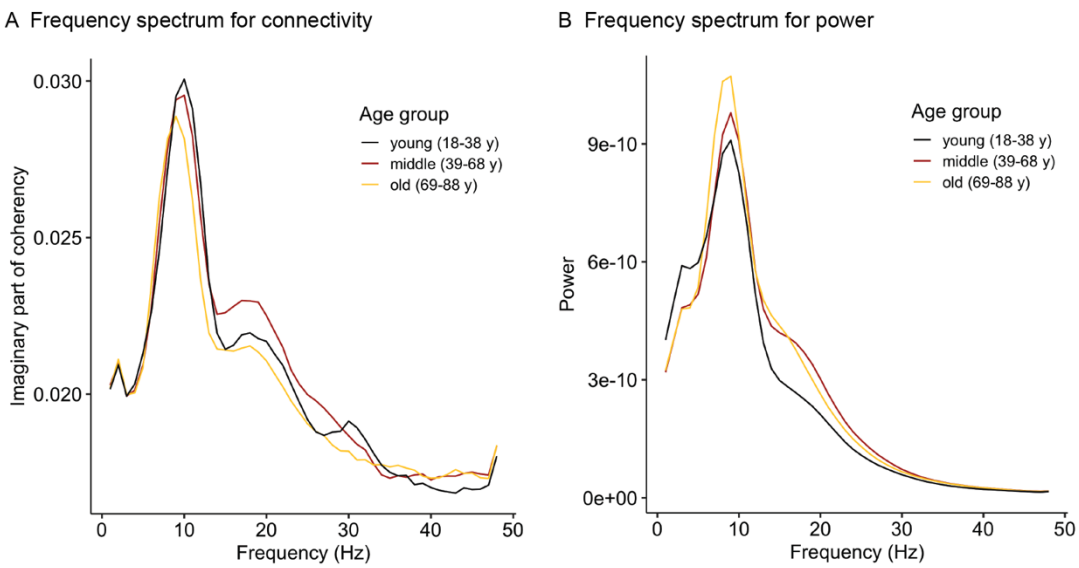

Fig. S1. Spectra for connectivity and power across age groups

For each individual included in this study, global connectivity or power was computed for 1 Hz frequency bins and averaged for the corresponding age group (n_{young} = 100, n_{middle} = 150, n_{old} = 100). Black colors represent the young age group, red represents the middle age group, and light colors indicate the old age group.

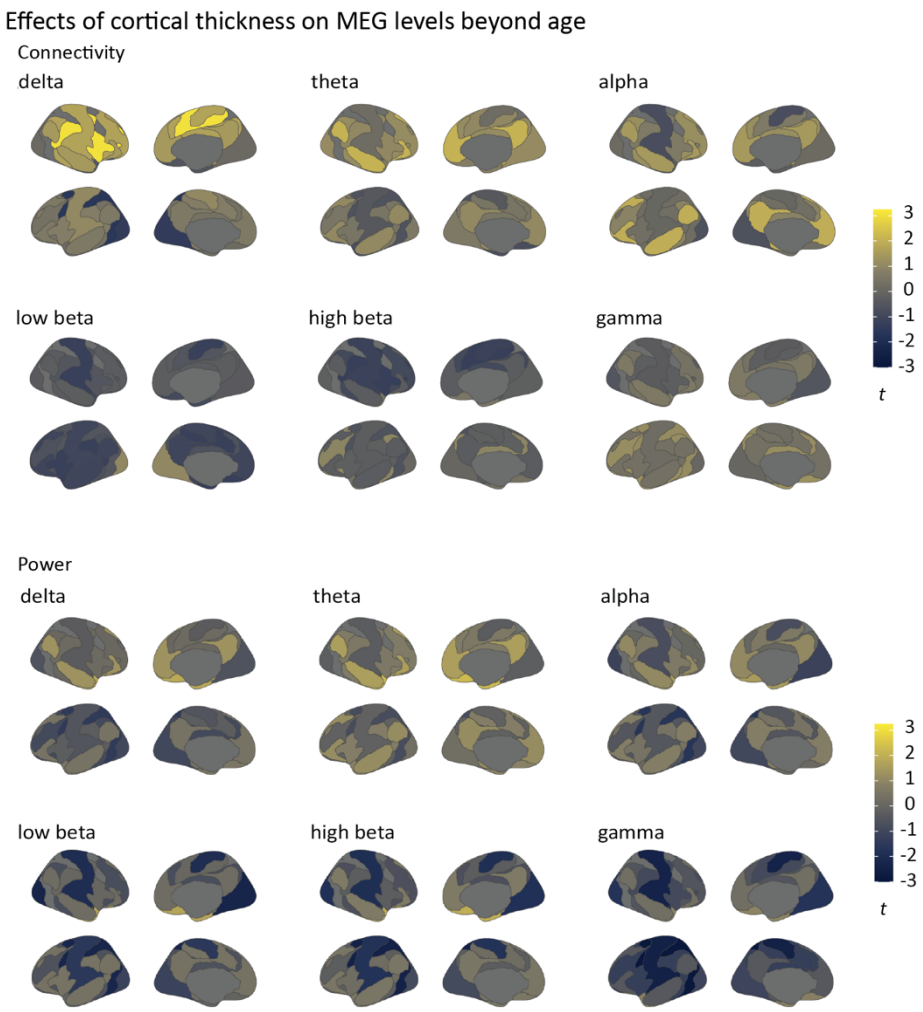

Fig. S2. Full t-value maps for the effect of cortical thickness on MEG levels across the adult lifespan sample

Shown is the influence of cortical thickness on functional MEG markers (t-values) across the whole study sample after regressing out the effects of covariables. We estimated general linear models including cortical thickness, age, age^2, sex, and total intracranial volume as independent variables and employed a statistical permutation framework to the models at the level of functional resting-state networks, as described in Yeo*, et al.* (1). Please see the main manuscript for the results after significance testing.

Table S1. Demographic data of the individual age groups included in the study

		Age (years)	Sex
Age group	*N*	Mean ± SD	Males : females
18-28 years	50	24.4 ± 3.4	25 : 25
29-38 years	50	33.3 ± 2.9	25 : 25
39-48 years	50	43.6 ± 3.0	25 : 25
49-58 years	50	53.7 ± 2.8	25 : 25
59-68 years	50	63.0 ± 2.8	25 : 25
69-78 years	50	71.8 ± 2.9	25 : 25
79-88 years	50	81.5 ± 2.7	25 : 25

Table S2. Relationship between global connectivity and age

	Contrast	t	p	$r_{partial}$
Delta	Age positive	1.50	0.106	0.08
	Age negative	-1.50	0.934	-0.08
	Age^2 convex	0.46	0.356	0.02
	Age^2 concave	-0.46	0.684	-0.02
	Sex	-0.79	0.790	-0.04
	Intracranial volume	0.69	0.240	0.04
Theta	Age positive	3.18	0.001*	0.17
	Age negative	-3.18	1.000	-0.17
	Age^2 convex	0.90	0.196	0.05
	Age^2 concave	-0.90	0.822	-0.05
	Sex	1.24	0.112	0.07
	Intracranial volume	4.72	<0.001*	0.25
Alpha	Age positive	-1.74	0.976	-0.09
	Age negative	1.74	0.043*	0.09
	Age^2 convex	-0.12	0.536	-0.01
	Age^2 concave	0.12	0.452	0.01
	Sex	0.81	0.206	0.04
	Intracranial volume	3.71	0.001*	0.20
Beta1	Age positive	-1.56	0.950	-0.08
	Age negative	1.56	0.064	0.08
	Age^2 convex	-3.39	1.000	-0.18
	Age^2 concave	3.39	0.002*	0.18
	Sex	1.28	0.089	0.07
	Intracranial volume	1.52	0.067	0.08
Beta2	Age positive	-0.67	0.754	-0.04
	Age negative	0.67	0.238	0.04
	Age^2 convex	-3.94	1.000	-0.21
	Age^2 concave	3.94	<0.001*	0.21
	Sex	1.24	0.104	0.07
	Intracranial volume	0.84	0.200	0.04
Gamma	Age positive	2.20	0.013*	0.12
	Age negative	-2.20	0.992	-0.12
	Age^2 convex	0.44	0.346	0.02
	Age^2 concave	-0.44	0.668	-0.02
	Sex	-1.17	0.870	-0.06
	Intracranial volume	0.90	0.208	0.05

Results were obtained by permutation analyses of linear models with global connectivity (imaginary part of coherency) as independent variable and age, age^2, sex, and total intracranial volume as dependent variables. We estimated the effects for positive and negative associations between age and connectivity, as well as the convex (U-shaped) and concave (inverted U-shaped) quadratic relationship in each frequency band. $r_{partial}$ reflects the degree of association between connectivity and age at which the influence of the other effects was eliminated.

Values of ± 0.1 reflect a small effect, ± 0.3 represent a moderate effect, and ± 0.5 is a large effect (2). The included healthy individuals (n = 350) ranged in age from 18 to 88 years. * denotes statistical significance at $p < 0.05$.

Table S3. Relationship between global power and age

	Contrast	*t*	*p*	$r_{partial}$
Delta	Age positive	-1.97	0.968	-0.11
	Age negative	1.97	0.021*	0.11
	Age^2 convex	3.50	0.003*	0.19
	Age^2 concave	-3.50	1.000	-0.19
	Sex	0.82	0.216	0.04
	Intracranial volume	4.79	<0.001*	0.25
Theta	Age positive	2.34	0.007*	0.12
	Age negative	-2.34	0.984	-0.12
	Age^2 convex	1.94	0.038*	0.10
	Age^2 concave	-1.94	0.980	-0.10
	Sex	1.30	0.089	0.07
	Intracranial volume	5.19	<0.001*	0.27
Alpha	Age positive	2.77	0.006*	0.15
	Age negative	-2.77	0.996	-0.15
	Age^2 convex	-0.09	0.520	0.00
	Age^2 concave	0.09	0.472	0.00
	Sex	0.12	0.460	0.01
	Intracranial volume	4.56	<0.001*	0.24
Beta1	Age positive	4.88	<0.001*	0.25
	Age negative	-4.88	1.000	-0.25
	Age^2 convex	-1.83	0.970	-0.10
	Age^2 concave	1.83	0.031*	0.10
	Sex	0.56	0.288	0.03
	Intracranial volume	2.79	0.003*	0.15
Beta2	Age positive	3.66	<0.001*	0.19
	Age negative	-3.66	1.000	-0.19
	Age^2 convex	-4.21	1.000	-0.22
	Age^2 concave	4.21	0.001*	0.22
	Sex	0.68	0.272	0.04
	Intracranial volume	2.62	0.006*	0.14
Gamma	Age positive	4.62	<0.001*	0.24
	Age negative	-4.62	1.000	-0.24
	Age^2 convex	-3.14	0.996	-0.17
	Age^2 concave	3.14	<0.001*	0.17
	Sex	-0.06	0.592	0.00
	Intracranial volume	1.72	0.050	0.09

Results were obtained by permutation analyses of linear models with global power as independent variable and age, age^2, sex, and total intracranial volume as dependent variables. We estimated the effects for positive and negative associations between age and power as well as the convex (U-shaped) and concave (inverted U-shaped) quadratic relationship in each frequency band. $r_{partial}$ reflects the degree of association between power and age at which the influence of the other effects was eliminated. Values of ± 0.1 reflect a small effect, ± 0.3 represent a

moderate effect, and ± 0.5 is a large effect (2). The included healthy individuals (n = 350) ranged in age from 18 to 88 years. * denotes statistical significance at $p < 0.05$.

Table S4. Summary of interaction effects sex by age on global MEG metrics

		Connectivity		Power	
	Contrast	*t*	*p*	*t*	*p*
Delta	Sex*age positive	-1.24	0.882	-2.77	0.996
	Sex*age negative	1.24	0.108	2.77	0.007*
	Sex*age^2 convex	-2.06	0.988	0.42	0.318
	Sex*age^2 concave	2.06	0.017*	-0.42	0.672
Theta	Sex*age positive	0.76	0.204	-1.54	0.928
	Sex*age negative	-0.76	0.762	1.54	0.064
	Sex*age^2 convex	0.55	0.286	0.52	0.280
	Sex*age^2 concave	-0.55	0.686	-0.52	0.698
Alpha	Sex*age positive	0.85	0.200	-0.76	0.752
	Sex*age negative	-0.85	0.772	0.76	0.234
	Sex*age^2 convex	-1.49	0.932	0.13	0.448
	Sex*age^2 concave	1.49	0.062	-0.13	0.578
Beta1	Sex*age positive	0.74	0.240	-0.71	0.768
	Sex*age negative	-0.74	0.772	0.71	0.246
	Sex*age^2 convex	0.32	0.362	0.04	0.458
	Sex*age^2 concave	-0.32	0.614	-0.04	0.558
Beta2	Sex*age positive	-1.14	0.908	-0.73	0.784
	Sex*age negative	1.14	0.130	0.73	0.240
	Sex*age^2 convex	-0.14	0.564	-0.02	0.504
	Sex*age^2 concave	0.14	0.390	0.02	0.526
Gamma	Sex*age positive	-0.55	0.694	-0.19	0.544
	Sex*age negative	0.55	0.300	0.19	0.418
	Sex*age^2 convex	1.43	0.068	-0.14	0.534
	Sex*age^2 concave	-1.43	0.916	0.14	0.420

Results were obtained by permutation analyses of linear models testing whether the coefficients for the age and age^2 effect on MEG metrics differed between males ($n = 175$) and females ($n = 175$) after correcting for the influence of total intracranial volume. Positive and negative linear associations between age and the metrics as well as the convex (U-shaped) and concave (inverted U-shaped) quadratic relationship in each frequency band were considered. The included healthy individuals ($n = 350$) ranged in age from 18 to 88 years. * denotes statistical significance at $p < 0.05$.

Table S5. Correlation between (negative) linear age effects on cortical thickness and MEG markers

	Metric	Age effect	r_s	p_{spin}
Delta	Connectivity	Linear (positive)	.343	0.004*
	Connectivity	Quadratic (convex)	.100	0.561
	Power	Linear (negative)	.314	0.008*
	Power	Quadratic (convex)	- .014	0.961
Theta	Connectivity	Linear (positive)	.030	0.932
	Connectivity	Quadratic (concave)	.205	0.351
	Power	Linear (positive)	- .028	0.935
	Power	Quadratic (convex)	- .152	0.568
Alpha	Connectivity	Linear (negative)	.012	0.967
	Connectivity	Quadratic (convex)	.220	0.095
	Power	Linear (positive)	.183	0.499
	Power	Quadratic (convex)	- .243	0.249
Beta1	Connectivity	Linear (negative)	- .015	0.963
	Connectivity	Quadratic (concave)	.227	0.197
	Power	Linear (positive)	.303	0.104
	Power	Quadratic (concave)	.431	0.007*
Beta2	Connectivity	Linear (negative)	- .181	0.581
	Connectivity	Quadratic (concave)	.267	0.253
	Power	Linear (positive)	.275	0.139
	Power	Quadratic (concave)	.479	0.002*
Gamma	Connectivity	Linear (positive)	- .051	0.851
	Connectivity	Quadratic (convex)	- .052	0.781
	Power	Linear (positive)	.093	0.495
	Power	Quadratic (convex)	- .366	0.077

Correlation analyses were performed between the age effect t statistics on cortical thickness and those on MEG markers at the vertex-level. Statistical significance of the correlation coefficients was tested using 10,000 random rotations (spin test; Alexander-Bloch, *et al.* (3). Significant correlations (p_{spin} < 0.05) suggest spatial correspondence of MEG alterations with cortical thinning across the lifespan (r_s = Spearman rank correlation coefficient; r_s < .3 indicates a weak, r_s from .3 to .5 indicates a moderate relationship (2).

Table S6. Correlation between quadratic age effects (concave) on cortical thickness and MEG markers

	Metric	Age effect	r_s	p_{spin}
Delta	Connectivity	Linear (positive)	.053	0.719
	Connectivity	Quadratic (convex)	- .218	0.028*
	Power	Linear (negative)	- .016	0.855
	Power	Quadratic (convex)	.113	0.543
Theta	Connectivity	Linear (positive)	.298	0.086
	Connectivity	Quadratic (concave)	- .049	0.771
	Power	Linear (positive)	.289	0.109
	Power	Quadratic (convex)	.147	0.441
Alpha	Connectivity	Linear (negative)	.295	0.050
	Connectivity	Quadratic (convex)	- .109	0.313
	Power	Linear (positive)	.121	0.553
	Power	Quadratic (convex)	.107	0.548
Beta1	Connectivity	Linear (negative)	.360	0.024*
	Connectivity	Quadratic (concave)	.193	0.118
	Power	Linear (positive)	.005	0.975
	Power	Quadratic (concave)	- .065	0.727
Beta2	Connectivity	Linear (negative)	.218	0.386
	Connectivity	Quadratic (concave)	- .144	0.441
	Power	Linear (positive)	- .012	0.936
	Power	Quadratic (concave)	- .174	0.321
Gamma	Connectivity	Linear (positive)	.027	0.897
	Connectivity	Quadratic (convex)	<.001	0.996
	Power	Linear (positive)	.038	0.671
	Power	Quadratic (convex)	.171	0.351

Correlation analyses were performed between the age effect t statistics on cortical thickness and those on MEG markers at the vertex-level. Statistical significance of the correlation coefficients was tested using 10,000 random rotations (spin test; Alexander-Bloch, *et al.* (3). Significant correlations (p_{spin} < 0.05) suggest spatial correspondence of MEG and cortical thickness alterations across the lifespan (r_s = Spearman rank correlation coefficient; r_s < .3 indicates a weak, r_s from .3 to .5 indicates a moderate relationship (2).

SI References

1. B. T. Yeo *et al.*, The organization of the human cerebral cortex estimated by intrinsic functional connectivity. *Journal of neurophysiology* (2011).
2. A. Field, J. Miles, Z. Field (2012) Discovering statistics using R. (Sage London).
3. A. F. Alexander-Bloch *et al.*, On testing for spatial correspondence between maps of human brain structure and function. *Neuroimage* **178**, 540-551 (2018).